Environmental Science & Technology

Supporting Information

Macroscopic and spectroscopic assessment of the co-sorption of Fe(II) with As(III) and As(V) on Al-oxide

Ying Zhu and Evert J. Elzinga

Department of Earth & Environmental Sciences, Rutgers University, Newark, NJ, USA

12 pages, 9 Figures, 2 Tables

1. EXAFS data analyses of the sorption samples and reference compounds

EXAFS data fitting of the spectra was done on Fourier transformed k^3 weighed χ spectra in R-space using WinXAS 3.1 [1]. Theoretical backscattering paths of Fe-O, Fe-Fe and Fe-Al were calculated with the FEFF 7.0 code [2], based on the structure of nikischerite (a Fe(II)-Al(III)-LDH with chemical formula $NaFe^{II}_6\ Al_3(SO_4)_2(OH)_{18}\ (H_2O)_{12}$, characterized in reference [3]), whereas Fe-As, As-O, As-Fe single scattering and three multiple scattering (MS) within the As(V) centered tetrahedron was calculated based on the structure of scorodite ($Fe(III)As(V)O_4 \cdot 2H_2O$, characterized in reference [4]). Theoretical As-Al scattering paths were obtained by replacing Fe with Al in octahedral positions of scorodite. The amplitude reduction factor was set at 0.9 for the Fe fits, and at 1.0 for the As fits. A single E_0 shift value was allowed to vary during optimization.

The Fe *K*-edge EXAFS data of samples containing Fe(II)-Al(III)-LDH were fitted with three paths: first-shell Fe-O, and second-shell Fe-Fe and Fe-Al, based on the crystal structure of nikischerite.[3] In this structure, Fe(II) is surrounded by six first-shell O atoms, and three Fe and three Al second-shell neighbors that are located at the same radial distance (Figure S1). To reduce the number of free parameters, the radial distances and Debye-Waller factors (σ^2) of second-shell Fe-Fe and Fe-Al were constrained to be the same, while all other factors were allowed to vary. For the aqueous Fe(II) reference and the dual-sorbate samples containing 0.5 mM As(V), only first-shell Fe-O was fitted due to the lack of apparent second-neighbor backscattering as observed in the RSFs (Figure 3 of the main manuscript). The spectrum of the Fe(II)-As(V) precipitate was fitted with first-shell Fe-O and second-shell Fe-Fe and Fe-As paths.

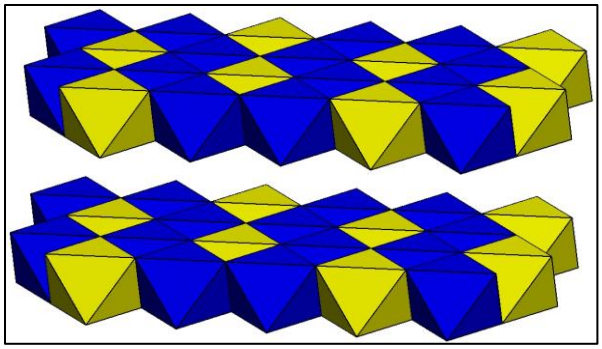

Figure S1: The structure of nikischerite, a Fe(II)-Al(III)-LDH mineral with chemical formula $NaFe^{II}_6\ Al_3(SO_4)_2(OH)_{18}\ (H_2O)_{12}$. Blue and yellow octahedra represent Fe(II) and Al(III) cations in octahedral coordination with hydroxyl groups respectively. The octahedral layers have a positive structural charge, which is balanced by sulfate anions in the interlayer (not shown).

The As *K*-edge EXAFS data of all the sorption samples were fitted with first-shell O backscatters and second-shell Al backscatters. For As(V) sorption samples in both binary and ternary systems, three fully restrained MS paths within the As(V) centered tetrahedron were also employed in the fitting, in addition to As-O and As-Al paths alone (results not shown), following the MS fitting scheme of Mikutta et al.[5] and Voegelin et al.[6] The inclusion of MS slightly improved the fitting quality without inducing substantial changes in the major parameters of As-O and As-Al distances, which agrees with the findings of Voegelin et al.[6] Because of the minor impacts of MS on our fitting results and data interpretation, only the single-shell fits are presented in Table S1, consistent with other studies (e.g. reference [7]). For the As data of the ternary sorption samples, we also tested data fits assuming As-Fe instead of As-Al second-neighbor scattering. This yielded distinctly worse fit quality relative to fits with second-neighbor As-Al scattering, regardless of the inclusion of MS paths. This confirms our interpretation of As being present as adsorption complexes at the Al-oxide surface in both the presence and absence of Fe(II), as discussed in the main manuscript. For the aqueous arsenite and arsenate references,

only first-shell O was fitted, while for the reference Fe(II)-As(V) precipitate, first-shell As-O and second-shell As-Fe paths were fitted (Table S2).

Error estimates of the optimized XAS fitting parameters are ±0.02 Å for the radial distance (R) of the first coordination shells, and ±0.04 Å for the radial distances of longer shells. For coordination numbers (CN), which are correlated to the Debye-Waller factor, the estimated error is ± 25 %. These error estimates of the fitting parameters are based on fits of reference compounds and estimates provided in previous relevant XAS studies. [7-11]

2. Comparison of structural information of symplesite and EXAFS fit results of the Fe(II)-As(V) reference precipitate

Figure S2 shows the mineralogical structure of symplesite ($Fe_3(AsO_4)_2 \cdot 8H_2O$), which is crystallographically similar to vivianite ($Fe_3(PO_4)_2 \cdot 8H_2O$), [12] reflecting the chemical similarity of arsenate and phosphate. The structure of symplesite contains single $Fe^{II}O_6$ octahedra and pairs of edge sharing Fe(II) octahedra (double Fe(II) octahedra), which are linked by arsenate groups (Figure S2). The structural arrangement of Fe(II) and As(V) is further resolved in Figure S3. Based on experimental distance of Fe-O (2.10-2.14 Å) and As-O (1.68-1.69 Å), and Fe-O-As angles provided in Figure S3, theoretical bond distance of Fe-As was estimated to be 3.43-3.56 Å.

Our EXAFS data fitting results (Table S1) of the Fe(II)-As(V) precipitate indicate that it is structurally similar to symplesite. The Fe *K*-edge EXAFS fitting results of Fe(II)-As(V)-precipitate (Table S1), the first shell is fitted with 5.3 O atoms at a radial distance of 2.11 Å, in agreement with an octahedral arrangement of O atoms around central Fe(II). The second-shell $R_{Fe\text{-}Fe}$=3.25 Å is very close to the Fe-Fe distance (3.26 Å) in $Fe(OH)_2$,[13] consistent with the edge-sharing octahedron configuration for double Fe(II) groups present in symplesite (Figure S2 and

S3b, S3c). In addition, the average R_{Fe-As}=3.45 Å is within the range of estimated Fe-As distance in symplesite, as shown above. The As *K*-edge EXAFS fitting results show first-shell CN_{As-O}= 3.3(±30%) for Fe(II)-As(V) precipitate at an average distance of R = 1.68 Å, suggesting that As(V) is coordinated by O atoms in tetrahedral configuration [7, 14-16]. The second-shell R_{As-Fe} = 3.41 Å is consistent with the average R_{Fe-As} obtained from Fe *K*-edge EXAFS results, given the large error of ±0.04 Å correlated with R values of second-shell fitting. This result is also within the range of As-Fe distance of 3.31-3.55 Å reported in Jönsson and Sherman (2008).[17]

Although the EXAFS fitting results demonstrate reasonable similarity between the structure of the Fe(II)-As(V) bulk precipitate and symplesite, XRD analysis showed the material to be amorphous precluding confirmation of phase identity and purity.

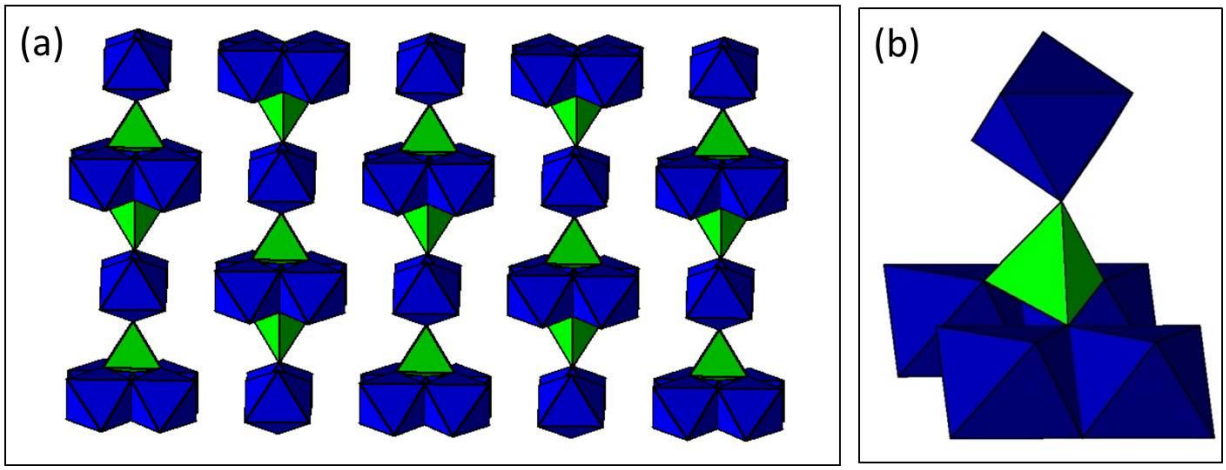

Figure S2: (a) Structure of symplesite ($Fe_3(AsO_4)_2 \cdot 8H_2O$);[12] (b) arsenate tetrahedron coordinated with 1 single Fe(II) octrahedron and 2 pairs of double Fe(II) octrahedra. Blue octahedra and green tetrahedra represent octahedral Fe(II) and tetrahedral As(V), respectively.

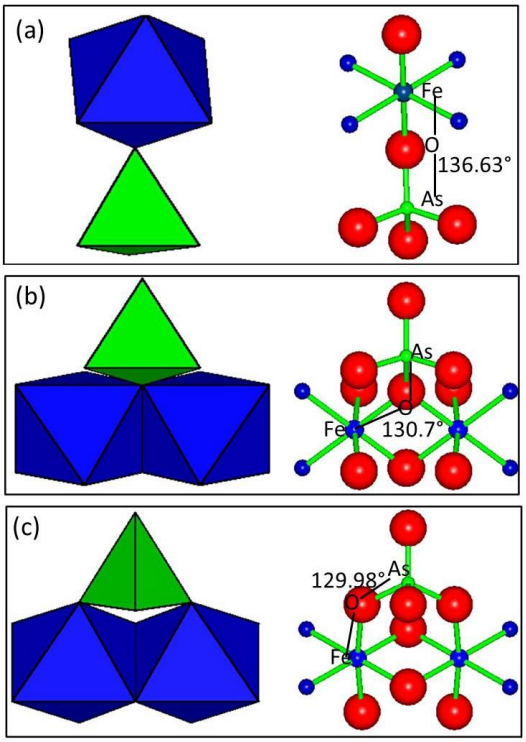

Figure S3: Arrangement of As(V) and Fe(II) within the symplesite structure presented by polyhedra (left) and atomic spheres (right): (a) As(V) tetrahedron coordinated with a single Fe(II) octahedron; (b)(c) As tetrahedron link with a double Fe(II) octahedral unit. Red, green, big blue and small blue atomic spheres in the right represent oxygen, As, Fe and water, respectively. Fe-O-As angles[12] used for distance calculation are indicated in each figure.

3. As *K*-edge EXAFS data of sorption samples and As reference compounds

Figures S4- S7 present the entire set of As *K*-edge EXAFS data collected for this study; the fit results are presented in Table S2. The first peak in the RSFs represents the first-shell O atoms surrounding central As(V) and As(III). The second shells visible in the RSFs of the sorption samples represent second-shell Al neighbors in the coordination sphere of sorbed As(III) and As(V), consistent with inner-sphere coordination of both arsenic species at the Al-oxide surface.

The spectral comparison presented in Figure S8 illustrates that the dominant As(V) sorption mechanism on γ-Al_2O_3 remains the same, irrespective of the initial As(V) concentrations. The comparison displayed in Figure S9 shows the similarity of the speciation of As(III) and As(V) in single- and dual-sorbate systems. This demonstrates that Fe(II) has no noticeable impact on the mode of As retention in our experimental systems, with both As(III) and As(V) coordinated predominantly as bidentate binuclear adsorption complexes at the surface of the Al-oxide sorbent in both the presence and absence of Fe(II).

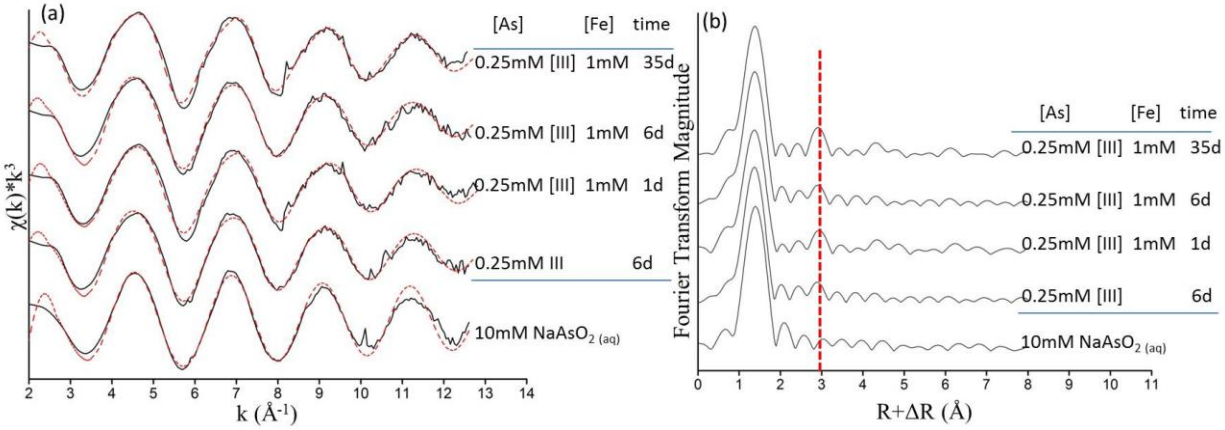

Figure S4: As *K*-edge EXAFS spectra of aqueous As(III) and As(III)/γ-Al_2O_3 sorption samples in single-sorbate reaction and dual-sorbate reactions with 1mM Fe(II) addition: (a) k^3-weighted χ spectra and (b) corresponding radial structure functions (RSFs). Solid and red dotted lines in panel (a) represent raw and fitted spectra, respectively. The red vertical dashed line in panel (b) locates the second-shell Al neighbors in the sorption samples.

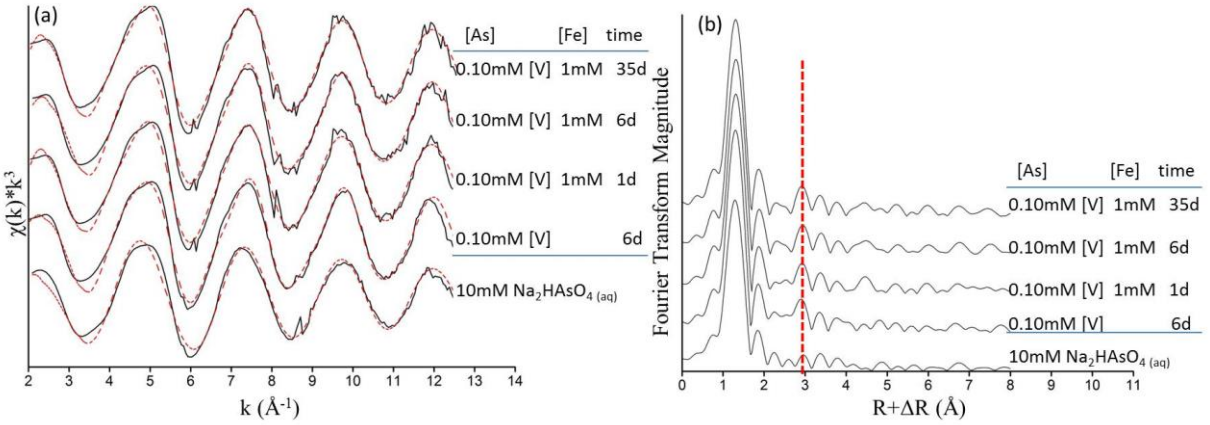

Figure S5: As *K*-edge EXAFS spectra of aqueous As(V) and 0.1mM As(V)/γ-Al_2O_3 sorption products in single-sorbate reaction and dual-sorbate reactions with 1mM Fe(II) addition: (a) k^3-weighted χ spectra and (b) corresponding radial structure functions (RSFs). Solid and red dotted lines in panel (a) represent raw and fitted spectra, respectively. Red vertical dashed line in panel (b) indicates second-shell As-Al backscatters in the sorption samples.

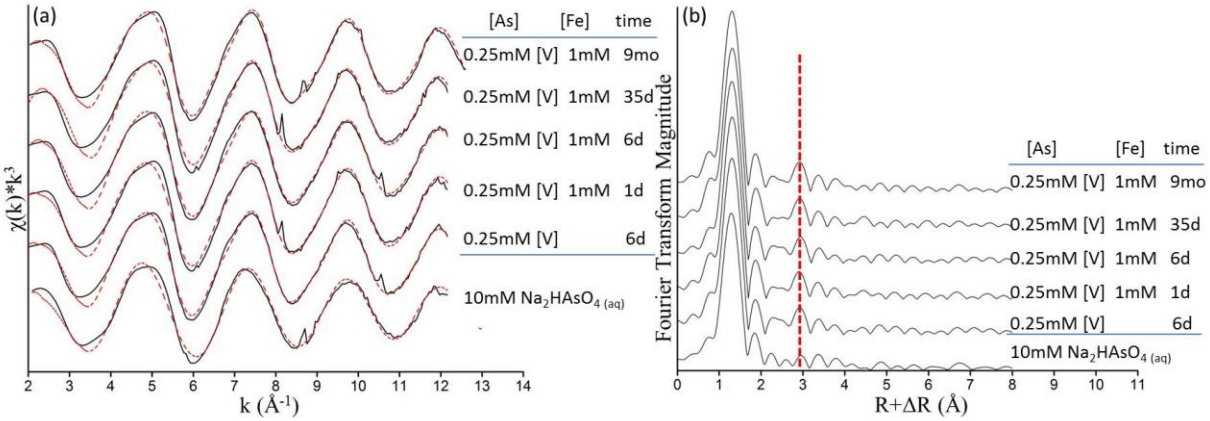

Figure S6: As *K*-edge EXAFS spectra of aqueous As(V) and 0.25mM As(V)/γ-Al_2O_3 sorption products in single-sorbate reaction and dual-sorbate reactions with 1mM Fe(II) addition: (a) k^3-weighted χ spectra and (b) corresponding radial structure functions (RSFs). Solid and red dotted lines in panel (a) represent raw and fitted spectra, respectively. Red vertical dashed line in panel (b) indicates second-shell As-Al backscatters in the sorption samples.

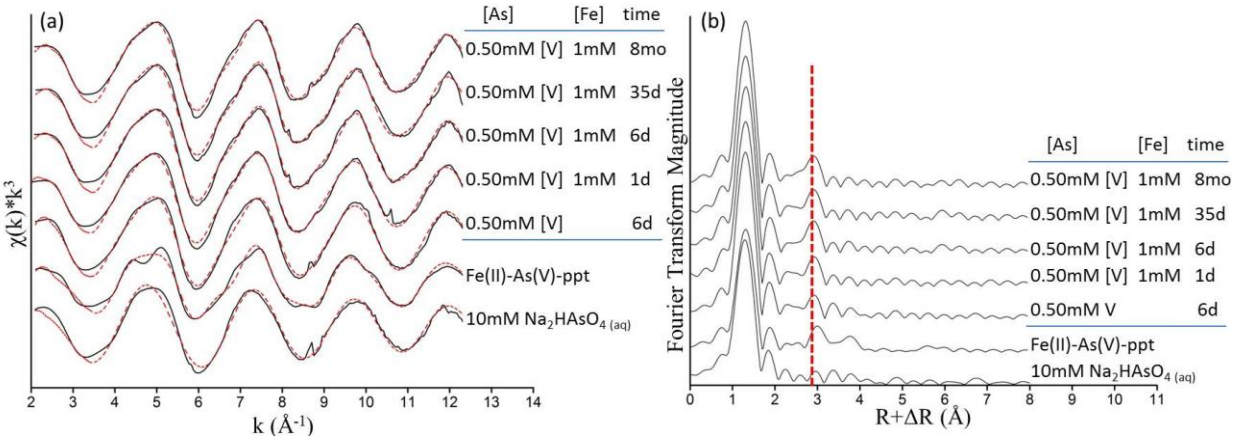

Figure S7: As *K*-edge EXAFS spectra of aqueous As(V) and 0.50mM As(V)/γ-Al_2O_3 sorption products in single-sorbate reaction and dual-sorbate reactions with 1mM Fe(II) addition: (a) k^3-weighted χ spectra and (b) corresponding radial structure functions (RSFs). Solid and red dotted lines in panel (a) represent raw and fitted spectra, respectively. Red vertical dashed line in panel (b) indicates second-shell As-Al backscatters in the sorption samples.

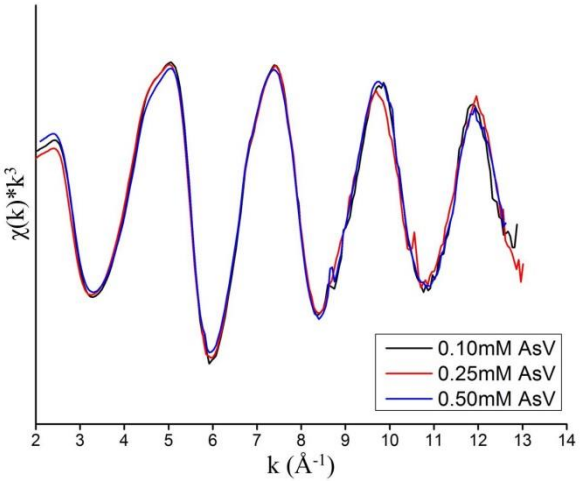

Figure S8: Comparison of the k^3-weighted χ spectra of As(V) reacted γ-Al_2O_3 single-sorbate sorption samples with various As(V) concentration for a reaction time of 6 days.

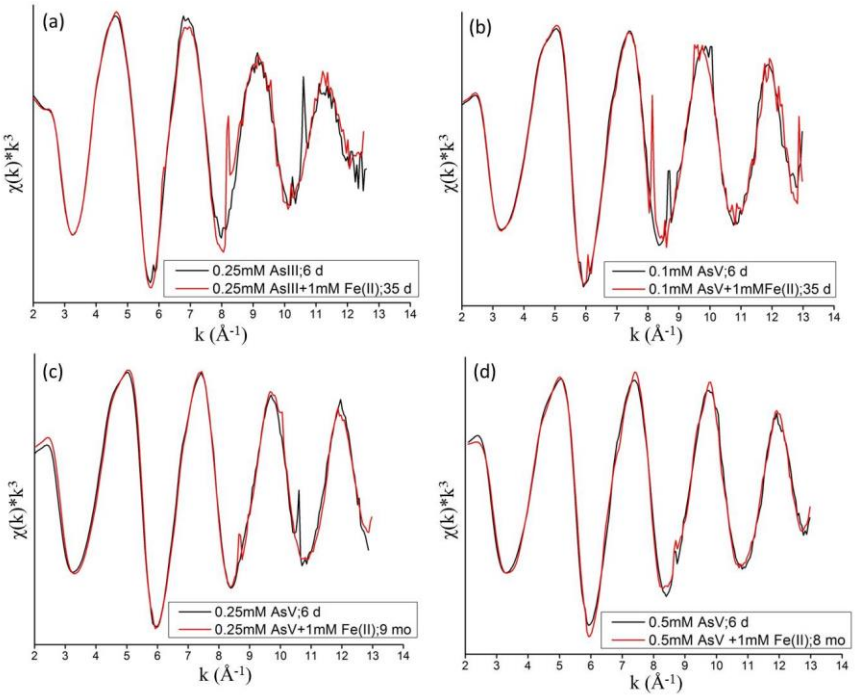

Figure S9: Comparison of the k^3-weighted As χ spectra of As reacted γ-Al_2O_3 single-sorbate and dual-sorbate sorption samples, with different As speciation and concentrations: (a) 0.25mM As(III); (b) 0.10mM As(V); (c) 0.25mM As(V); (d) 0.50mM As(V).

Table S1. Fe *K*-edge EXAFS Fitting Results of Fe(II) Sorption and Reference Samples

sorption samples				Fe-O			Fe-Fe			Fe-Al			Fe-As		
$[Fe]_0$	$[As]_0$	time	Γ[d]	CN[a]	R (Å)[b]	σ^2 (Å^2)[c]	CN	R (Å)	σ^2 (Å^2)	CN	R (Å)	σ^2 (Å^2)	CN	R (Å)	σ^2 (Å^2)
1mM	0.50mM V	8 mo	1.96	5.8	2.10	0.010									
1mM	0.50mM V	35 d	2.36	5.3	2.09	0.010									
1mM	0.50mM V	6 d	1.76	5.4	2.10	0.010									
1mM	0.50mM V	1 d	1.70	6.0	2.09	0.012									
1mM	0.25mM V	9 mo	2.19	5.7	2.11	0.009	3.6	3.14	0.010	2.9	3.14	0.010			
1mM	0.25mM V	35 d	1.53	5.5	2.10	0.009	2.6	3.13	0.010	2.3	3.13	0.010			
1mM	0.25mM V	6 d	0.95	5.0	2.09	0.009									
1mM	0.25mM V	1 d	0.83	4.8	2.08	0.010									
1mM	0.10mM V	35 d	1.97	6.0	2.11	0.009	4.2	3.14	0.010	2.9	3.14	0.010			
1mM	0.10mM V	6 d	1.33	5.2	2.11	0.009	3.0	3.15	0.010	2.4	3.15	0.010			
1mM	0.10mM V	1 d	0.80	5.0	2.08	0.009									
1mM	0.25mM III	6 d	1.81	6.0	2.11	0.008	4.0	3.14	0.009	2.6	3.14	0.009			
1mM	0.25mM III	1 d	1.02	5.7	2.1	0.008	3.7	3.13	0.009	2.8	3.13	0.009			
1mM	—	6 d	1.83	5.8	2.12	0.008	4.8	3.15	0.010	2.0	3.15	0.010			
1mM	—	1 d	1.07	6.0	2.12	0.009	4.0	3.15	0.010	2.3	3.15	0.010			
1mM	—	2 hr	0.50	6.0	2.12	0.009	4.2	3.15	0.010	2.4	3.15	0.010			
Fe references															
Nikischerite				5.5	2.13	0.007	4.0	3.15	0.009	2.3	3.15	0.009			
aqueous Fe^{2+}				5.7	2.11	0.010									
Fe(II)As(V)-precipitate				5.4	2.11	0.008	0.9	3.25	0.015				3.5	3.45	0.015

[a] CN is coordination number; [b] R is interatomic radial distance; [c] σ^2 is Debye-Waller factor. Error estimates and details on fitting procedure are described above in section 1 above. [d] Γ is the Fe(II) sorption density (μmol/m^2) calculated based on the N_2-BET surface area.

Table S2. As *K*-edge EXAFS Fitting Results of As Sorption and Reference Samples

sorption samples				As-O			As-Al			As-Fe		
$[Fe]_0$	$[As]_0$	time	Γ[d]	CN[a]	R (Å)[b]	σ^2 (Å^2)[c]	CN	R (Å)	σ^2 (Å^2)	CN	R (Å)	σ^2 (Å^2)
1mM	0.50mM V	8 mo	1.42	4.1	1.68	0.002	3.3	3.14	0.006			
1mM	0.50mM V	35 d	1.42	4.1	1.69	0.002	3.2	3.15	0.006			
1mM	0.50mM V	6 d	1.41	4.2	1.69	0.002	3.2	3.14	0.006			
1mM	0.50mM V	1 d	1.39	4.3	1.69	0.002	2.7	3.14	0.006			
	0.50mM V	6 d	1.04	4.1	1.68	0.002	2.6	3.12	0.006			
1mM	0.25mM V	9 mo	0.71	4.4	1.68	0.002	2.8	3.14	0.006			
1mM	0.25mM V	35 d	0.71	4.1	1.69	0.002	2.5	3.15	0.006			
1mM	0.25mM V	6 d	0.70	4.3	1.68	0.002	2.4	3.13	0.006			
1mM	0.25mM V	1 d	0.68	4.5	1.68	0.003	2.5	3.13	0.006			
	0.25mM V	6 d	0.67	4.4	1.68	0.002	2.6	3.14	0.006			
1mM	0.10mM V	35 d	0.28	4.3	1.68	0.002	2.5	3.15	0.006			
1mM	0.10mM V	6 d	028	4.1	1.68	0.002	2.4	3.15	0.006			
1mM	0.10mM V	1 d	0.28	4.2	1.68	0.002	2.5	3.15	0.006			
	0.10mM V	6 d	0.26	4.2	1.68	0.002	2.7	3.13	0.006			
1mM	0.25mM III	35 d	0.48	3.2	1.77	0.004	1.6	3.22	0.009			
1mM	0.25mM III	6 d	0.42	3.5	1.78	0.004	1.3	3.24	0.009			
1mM	0.25mM III	1 d	0.38	3.2	1.77	0.004	1.6	3.22	0.009			
	0.25mM III	6 d	0.41	3.4	1.78	0.004	1.3	3.23	0.009			
As references												
10mM $Na_2HAs(V)O_{4(aq)}$				4.2	1.68	0.003						
10mM $NaHAs(III)O_{2(aq)}$				3.0	1.79	0.002						
Fe(II)-As(V)-precipitate				3.3	1.68	0.002				4.1	3.41	0.015

[a] CN is coordination number; [b] R is interatomic radial distance; [c] σ^2 is Debye-Waller factor; [d] Γ is the As(III/V) sorption density (μmol/m^2) calculated based on the N_2-BET surface area.

References

(1) Ressler, T. WinXAS : a new software package not only for the analysis of energy-dispersive XAS data. *J. Phys. IV France* **1997**, *7*, C2–C269.

(2) Ankudinov, A. L.; Rehr, J. J. Relativistic calculations of spin-dependent x-ray-absorption spectra. *Phys. Rev. B* **1997**, *56*, R1712–R1715.

(3) Huminicki, D. M. C.; Hawthorne, F. C. The crystal structure of nikischerite, $NaFe^{2+}{}_6Al_3(SO_4)_2(OH)_{18}(H_2O)_{12}$, a mineral of the shigaite group. *Can. Mineral.* **2003**, *41*, 79–82.

(4) Kitahama, K.; Kiriyama, R.; Baba, Y. Refinement of the Crystal Structure of Scorodite. *Acta Cryst.* **1975**, *B31*, 322–324.

(5) Mikutta, C.; Frommer, J.; Voegelin, A.; Kaegi, R.; Kretzschmar, R. Effect of citrate on the local Fe coordination in ferrihydrite, arsenate binding, and ternary arsenate complex formation. *Geochim. Cosmochim. Acta* **2010**, *74*, 5574–5592.

(6) Voegelin, A.; Weber, F. A.; Kretzschmar, R. Distribution and speciation of arsenic around roots in a contaminated riparian floodplain soil: Micro-XRF element mapping and EXAFS spectroscopy. *Geochim. Cosmochim. Acta* **2007**, *71*, 5804–5820.

(7) Arai, Y.; Elzinga, E. J.; Sparks, D. L. X-ray absorption spectroscopic investigation of arsenite and arsenate adsorption at the aluminum oxide-water interface. *J. Colloid Interface Sci.* **2001**, *235*, 80–88.

(8) Elzinga, E. J. Formation of layered Fe(II)-Al(III)-hydroxides during reaction of Fe(II) with aluminum oxide. *Environ. Sci. Technol.* **2012**, *46*, 4894–4901.

(9) Scheidegger, A. M.; Lamble, G. M.; Sparks, D. L. Spectroscopic evidence for the formation of mixed-cation hydroxide phases upon metal sorption on clays and aluminum oxides. *J. Colloid Interface Sci.* **1997**, *186*, 118–128.

(10) Elzinga, E. J.; Sparks, D. L. Reaction condition effects on nickel sorption mechanisms in illite–water suspensions. *Soil Sci. Soc. Am. J.* **2001**, *65*, 94–101.

(11) Roberts, D. R.; Ford, R. G.; Sparks, D. L. Kinetics and mechanisms of Zn complexation on metal oxides using EXAFS spectroscopy. *J. Colloid Interface Sci.* **2003**, *263*, 364–376.

(12) Mori, H.; Ito, T. The structure of vivianite and symplesite. *Acta Cryst.* **1950**, *3*, 1–6.

(13) Parise, J. B.; Marshall, W. G.; Smith, R. I.; Lutz, H. D.; Möller, H. The nuclear and magnetic structure of "white rust"— $Fe(OH_{0.86}D_{0.14})_2$. *Am. Mineral.* **2000**, *85*, 189–193.

(14) Alexandratos, V. G.; Elzinga, E. J.; Reeder, R. J. Arsenate uptake by calcite: macroscopic and spectroscopic characterization of adsorption and incorporation mechanisms. *Geochim. Cosmochim. Acta* **2007**, *71*, 4172–4187.

(15) Manning, B. A.; Fendorf, S. E.; Bostick, B.; Suarez, D. L. Arsenic(III) oxidation and arsenic(V) adsorption reactions on synthetic birnessite. *Environ. Sci. Technol.* **2002**, *36*, 976–981.

(16) Makris, K. C.; Sarkar, D.; Parsons, J. G.; Datta, R.; Gardea-Torresdey, J. L. X-ray absorption spectroscopy as a tool investigating arsenic(III) and arsenic(V) sorption by an aluminum-based drinking-water treatment residual. *J. Hazard. Mater.* **2009**, *171*, 980–986.

(17) Jönsson, J.; Sherman, D. M. Sorption of As(III) and As(V) to siderite, green rust (fougerite) and magnetite: implications for arsenic release in anoxic groundwaters. *Chem. Geol.* **2008**, *255*, 173–181.